Distribution of magnetic domain pinning fields in $Ga_{1-x}Mn_xAs$ ferromagnetic films

Jungtaek Kim, D. Y. Shin, and Sanghoon Lee*
Physics Department, Korea University, Seoul 136-701, Republic of Korea

X. Liu and J. K. Furdyna
Physics Department, University of Notre Dame, Notre Dame, Indiana 46556, USA
(Received 8 July 2008; published 7 August 2008)

The distribution of magnetic domain pinning fields was determined in ferromagnetic GaMnAs films using the angular dependence of the planar Hall effect. A major difference is found between the pinning field distribution in as-grown and in annealed films: the former showing a strikingly narrower distribution than the latter. This effect, which we ascribe to differences in the degree of uniformity of magnetic anisotropy, provides a better understanding of magnetic domain landscape in GaMnAs, a subject of current intense interest.

DOI: 10.1103/PhysRevB.78.075309 PACS number(s): 75.50.Pp, 75.30.Gw, 75.40.Gb

I. INTRODUCTION

The ferromagnetic semiconductor GaMnAs continues to be a subject of intense interest due to the opportunities that it holds out for spintronic applications.[1–3] Many of its physical properties, such as the effect of low-temperature annealing on the Curie temperature,[4–8] the role of Mn ions at interstitial positions,[7,9,10] and the dependence of magnetic anisotropy on strain and on carrier density, have been extensively investigated.[11–13] The uniformity of the magnetic phase in GaMnAs is still under debate. For example, the ac susceptibility measurements of Hamaya *et al.*[14] have led these authors to suggest a mixed magnetic phase model for GaMnAs. Wang *et al.*,[15] on the other hand, assumed a *single* uniform magnetic phase to interpret their ac susceptibility data on GaMnAs in terms of temperature-dependent changes in magnetic anisotropy. A major advancement in understanding the magnetic anisotropy has been made by Welp *et al.*,[16] who used magneto-optical imaging to map the magnetic domain structure in GaMnAs. This study demonstrated the coexistence of multiple domains with different magnetization directions during magnetization reversal. The magnetotransport measurements of Shin *et al.*[17] provided further evidence for presence of stable multidomain structures that form during magnetization reversal in GaMnAs.

In this paper we report a study of the magnetization reversal process in GaMnAs carried out by an alternative approach, i.e., by changing the *direction* of the applied magnetic field H while its magnitude is kept constant. It will be shown that this approach provides direct information on the distribution of pinning fields for a system comprised of multiple domains with different magnetization orientations.

II. SAMPLE FABRICATION AND EXPERIMENT PROCEDURE

A GaMnAs film with 6.2% of Mn and a thickness of 100 nm was used in this study. The details regarding growth, annealing, and sample preparation are described elsewhere.[18] Curie temperatures T_C of 62 and 136 K were estimated for the as-grown and annealed films from the temperature dependences of their respective resistivities. Planar Hall-effect (PHE) measurements revealed the magnetic easy axes lying in the layer plane in both samples but the magnetic anisotropy within the plane obtained from the angular dependence of PHE is found to be quite different in the two cases. The dependence of PHE on the orientation of **H** was measured as follows. The magnetization **M** of the sample was first saturated by applying a field of 4000 Oe at a given angle. The field was then reduced to the desired strength and PHE was measured as the direction of **H** rotated without changing the field strength. This procedure was repeated for a series of field strengths. The schematic for the Hall device together with crystallographic direction is shown in the inset of Fig. 4. The azimuthal angle was measured counterclockwise from the $[1\bar{1}0]$ direction (which is also the direction of the current).

III. RESULTS AND DISCUSSION

The angular dependences of the planar Hall resistance (PHR) obtained at several different magnetic fields for as-grown and annealed GaMnAs films are shown in Fig. 1. While under high magnetic fields, the PHR of both films shows a smooth sinusoidal-like behavior without hysteresis, indicative of *coherent* rotation. In the weak fields the PHR shows a clear hysteresis between clockwise (CW) and counterclockwise (CCW) rotations of the field, implying the presence of multidomain structures. Note that the PHR is strikingly different in as-grown and annealed films, showing an abrupt transition between its maximum $(+|k/tM^2|)$ and minimum $(-|k/tM^2|)$ values in the former, and a broad distributed transition region in the latter. These distinct hysteresis characteristics of the two films remained unchanged at different fields until the field strength reached saturation values. To understand this behavior, we start with the expression for the PHR for a single magnetic domain given by[19]

$$R_{\mathrm{PHR}} = \frac{k}{t} M^2 \sin 2\varphi_M, \tag{1}$$

where t is the film thickness, φ_M is the angle between the current and the magnetization **M**, and k is a constant related to the anisotropic magnetoresistance. The angular depen-

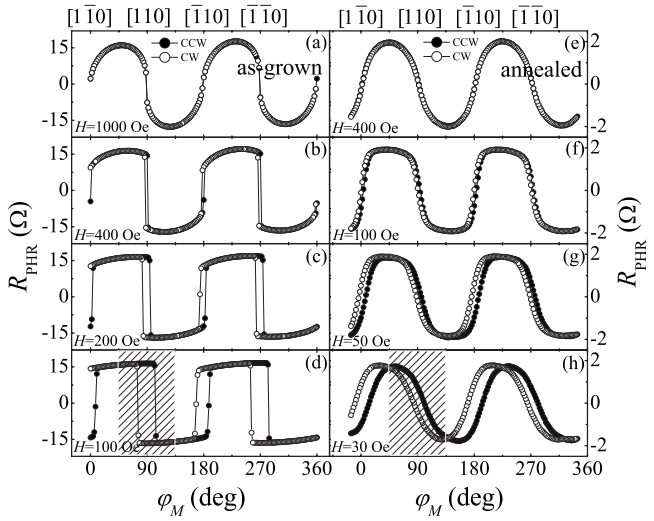

FIG. 1. Angular dependences of PHR data taken at several magnetic fields for as-grown (left column) and annealed (right column) GaMnAs films. The open and solid symbols show data taken with field rotations in CW and CCW directions, respectively. Note the striking hysteresis between the CW and CCW rotations observed at lower field values.

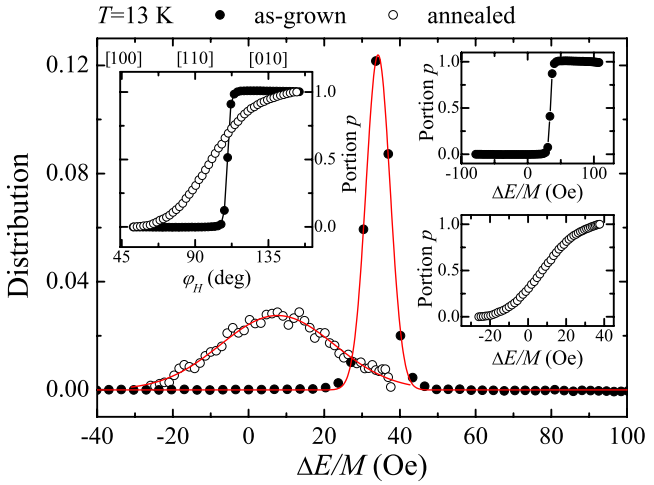

FIG. 2. (Color online) Probability of finding magnetic domains oriented along the [010] direction for a given pinning field. The widths of the distributions show clear contrast between as-grown (solid circles) and annealed (open circles) GaMnAs. The solid lines are Gaussian fits obtained with Eq. (4). The left-hand inset shows the fractional area p corresponding to magnetic domains with magnetization along [010] obtained from data in the shaded region of Fig. 1. The right-hand insets are plots of the relation between p and the pinning field $\Delta E/M$ mapped out from the data shown in the left inset.

dence of PHR (Refs. 18 and 20) for a multidomain structure can then be obtained by the sum of the contributions of individual domains given by Eq. (1).

To follow the changes in the domain structure during the rotation of **H**, we focus on the shaded transition region in Fig. 1 (which includes the point where **H** crosses the "hard" [110] axis). In this angular region **M** changes from the [100] direction to [010] via domain nucleation and propagation in a process similar to that discussed in Ref. 16. The value of the PHR reflects the sum of the fractions of the area occupied by domains oriented along [100] and [010] in the probed region near the leads. The resultant PHR reaches its minimum and maximum values, respectively, when the entire probed region reaches a single-domain state along one or the other of these directions.[17] The fractional area p corresponding to $\mathbf{M}\|[010]$ at any point during the transition from [100] to [010] (i.e., for CCW rotation of **H**) can be calculated from the relation $p=1/2(1-R_{\mathrm{PHR}}/R_{\mathrm{PHR}}^{\mathrm{max}})$ given in Ref. 21. The observed values of p are plotted in the left inset of Fig. 2.

The direction of **M** in an in-plane magnetized GaMnAs film is determined by the magnetic free energy, given by[22]

$$E = K_U \sin^2 \varphi_M + (K_C/4)\cos^2 2\varphi_M - MH\cos(\varphi_M - \varphi_H), \tag{2}$$

where H is the external magnetic field, K_U and K_C are uniaxial and cubic anisotropy coefficients, respectively, and φ_M and φ_H are angles of **M** and **H** measured from the [1$\bar{1}$0] direction, i.e., from the current direction. The free-energy difference between $\mathbf{M}\|[100]$ and $\mathbf{M}\|[010]$ is then

$$\Delta E = E_{[010]} - E_{[100]} = 2MH\cos\varphi_H \sin[(\varphi_M^{[010]} - \varphi_M^{[100]})/2], \tag{3}$$

where the orientations of $\mathbf{M}_{[100]}$ and $\mathbf{M}_{[010]}$ are denoted by the angles $\varphi_M^{[100],[010]}$. Note, however, that **M** may be slightly misaligned with either [100] or [010] both due to the presence of the external magnetic field and to contributions from uniaxial anisotropy.[23]

Since the energy difference ΔE between the two directions of **M** varies as $H\cos\varphi_H$ in Eq. (3), it can be continuously swept by varying the direction of **H**. This provides a direct handle for investigating the pinning energy[24] distribution of magnetic domains since only areas where the pinning energy is smaller than ΔE can make a transition $\mathbf{M}_{[100]}$ to $\mathbf{M}_{[010]}$ during the scan of ΔE. As the probed region of the sample breaks up into regions with the two different directions of **M**, the value of PHR changes to reflect the fractional areas corresponding to these two orientations. From the left inset of Fig. 2 (p vs φ_H) and Eq. (3) (ΔE vs φ_H), one can relate the fraction p to the value of $\Delta E/M$, as shown in the right insets of Fig. 2. Note that the relation between p and $\Delta E/M$ is a measure of the field strength required to reorient the domain magnetization from $\mathbf{M}_{[100]}$ to $\mathbf{M}_{[010]}$. The derivative of p with respect to $\Delta E/M$ then provides the probability of finding a domain with a pinning field $H_p=\Delta E/M$, which is the threshold external field required to cross the [110] direction. The probability distributions of such domain pinning fields are plotted for both samples in Fig. 2. This probability can be nicely fit by a Gaussian distribution

$$f(H_p) = \frac{1}{\sigma\sqrt{2\pi}}\exp\left[-\frac{(H_p - H_{\mathrm{avg}})^2}{2\sigma^2}\right], \tag{4}$$

where H_p is the pinning field for a domain with a given orientation of **M**, H_{avg} is the average pinning field over the entire ensemble of domains, and σ is the standard deviation of the pinning field fluctuation. These fits yield H_{avg} of

37.7 ± 0.4 Oe for the as-grown sample and 8.6 ± 0.3 Oe for the annealed sample. The pinning field distributions of two samples were obtained at several different temperatures using the same analysis. Although the mean values of pinning field distributions systematically decrease with increasing temperature, the shape of the distribution (i.e., the values of full width at half maximum) for the two samples remains nearly the same values below T_C, indicating that the broadness of the distribution is not caused by thermal fluctuations but originates from the intrinsic properties of the samples.

Figure 2 shows that the pinning field distribution for the as-grown specimen is confined to a very narrow region, indicating that domain pinning is quite homogeneous over the entire sample; i.e., the domains comprising the sample rotate coherently during magnetization reversal. This behavior is consistent with the uniform magnetic phase model adopted by Wang *et al.* for as-grown GaMnAs film.[15]

In contrast, Fig. 2 shows that, in the annealed sample, domain pinning fields are distributed over a broad region (even including a finite probability p for *negative* pinning fields). Such negative pinning fields are often observed in magnetic multilayers comprised of ferromagnetic (FM) and antiferromagnetic (AFM) layers, produced by exchange coupling between adjacent FM and AFM layers.[25] Our sample, however, consists of a single FM GaMnAs film so that the negative pinning field must have an entirely different origin.

To gain insight into the broad distribution of pinning energies in annealed GaMnAs (including negative values), we must reexamine the distribution of magnetic anisotropy within the sample. In the analysis presented above, we have assumed the entire film to be uniformly dominated by cubic anisotropy. However, magnetic domains in a GaMnAs film can in fact have different magnetic anisotropies, resulting in different magnetization directions at $H=0$. It is now well established that magnetic anisotropy in GaMnAs is a sensitive function of the hole concentration.[11,13] Small fluctuations of this parameter can then produce regions with different magnetic anisotropy (i.e., different relative strengths of K_U and K_C) and thus local variations of magnetic energy profiles, which result in a broad distribution of magnetic pinning fields, as is observed. The observation of negative pinning fields can also be understood in terms of this picture. If there are some areas dominated by uniaxial anisotropy along [110] and some by cubic anisotropy along ⟨100⟩, the magnetization in each of these areas will align according to energy minima determined by the magnetic anisotropy at zero field. As **M** makes the transition from $\mathbf{M}_{[100]}$ to $\mathbf{M}_{[010]}$, its relaxation toward $\mathbf{M}_{[110]}$ in uniaxial-anisotropy-dominated areas will appear as a rotation from $\mathbf{M}_{[100]}$ to $\mathbf{M}_{[010]}$ in a fraction of the sample. This will manifest itself as a negative pinning energy in the analysis used above where only transitions from $\mathbf{M}_{[100]}$ to $\mathbf{M}_{[010]}$ were considered.

To check whether there exists a distribution of different magnetic anisotropies in the annealed sample, we also compared field scans of PHR for the as-grown and the annealed films measured with different directions of **H**, as shown in the upper and lower panels of Fig. 3, respectively. The PHR of the annealed film changes significantly when the field is reduced toward zero even before its direction is reversed. This behavior is very different from what is observed in as-grown GaMnAs film with a strong cubic anisotropy, in which an abrupt change of PHR occurs only *after* the field direction is reversed.[16,20] Furthermore, in field scan experiments on annealed GaMnAs, the PHR at zero field is neither a maximum nor a minimum. This can only occur when the magnetization points along one of the in-plane ⟨100⟩ directions over the entire sample in the form of single domain.

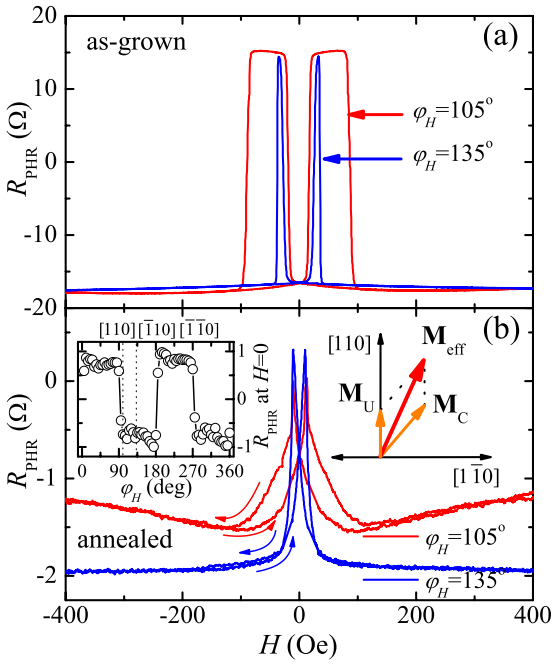

FIG. 3. (Color online) Representative field scans of PHR data obtained on as-grown (upper panel) and annealed (lower panel) GaMnAs films for field directions $\varphi_H=105°$ and $\varphi_H=135°$. Both scans of the annealed film show significant changes near zero field, giving the same intermediate value at the intercept. The zero-field intercepts obtained for PHR scans for the annealed film at different φ_H are given in the left-hand inset, showing that the transition occurs between two PHR values that correspond to a combination of two directions of magnetization, $\mathbf{M}\|[100]$ and $\mathbf{M}\|[010]$. This is illustrated in the right-hand inset where M_U and M_C indicate magnetizations dominated by uniaxial and cubic anisotropies, respectively. The dotted lines in the left inset indicate the filed angles, at which the representative field scans of PHR data are obtained.

Note also that PHR *consistently* returns to the *same* value at zero field, independent of what was the field direction during the scan. These observations directly suggest that some areas of the annealed sample are strongly dominated by uniaxial anisotropy along [110] and some by cubic anisotropy along the ⟨100⟩ directions. In such configuration the direction of the *average* magnetization at zero field will lie between these two orientations, as shown in the right-hand inset of Fig. 3. This will result in an intermediate value of PHR, exactly as is observed. Since this distribution of magnetic domains is intrinsic to a given film, it will result in the same value of PHR at zero field, independent of the **H** direction used during the scan. This is confirmed by the field angle data in the left-hand inset of Fig. 3, which shows that PHR changes only between two values that are both of the same magnitude (positive for the [100] and [110] combination; negative for [010] and [$\bar{1}$10]). This observation directly

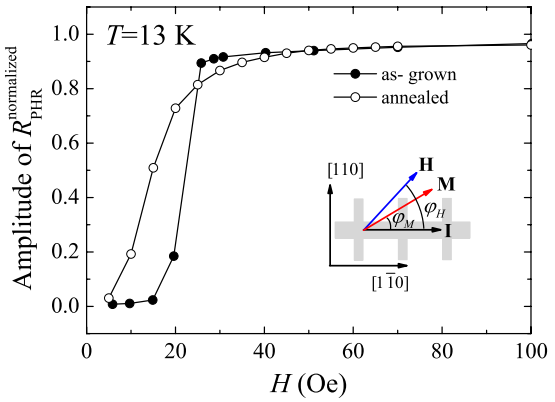

FIG. 4. (Color online) Magnetic field dependence of the maximum-to-minimum amplitude of PHR obtained from the angular dependence data. The solid and open circles correspond to as-grown and annealed samples. Note the striking difference between the behavior of the two materials at fields below 40 Oe (i.e., below saturation of M). The schematic of the Hall device used in the PHR measurements, together with crystallographic direction, is shown in the inset.

indicates that annealed GaMnAs consists of areas having different magnetic anisotropies, similar to the mixed magnetic phase model suggested by Hamaya *et al.*[14]

The above picture was further tested by investigating the process of magnetization reorientation for various field strengths. The field dependence of the amplitude of PHR, normalized by the PHR maximum at 4000 Oe, is shown in Fig. 4. The normalized PHR amplitude remains constant (close to unity) at fields above 40 Oe, indicating that above 40 Oe the magnetization in the entire sample follows the rotation of **H**. This is consistent with the domain pinning field distribution shown in Fig. 2 where the upper ends of the distributions lay around 40 Oe for both samples. At lower fields, however, PHR is clearly seen to decrease as the field is reduced since the areas having pinning fields larger than the applied field strength can no longer follow the rotation of the field. Thus the lower the field, the lesser fraction of the sample can respond to the field rotation. As seen in Fig. 4, in the as-grown sample the amplitude of PHR drops to zero within a very narrow field window while the decrease in PHR in the annealed sample is much more gradual. This behavior directly reflects the difference of domain pinning field distributions in the as-grown and the annealed GaMnAs.

IV. CONCLUSIONS

Based on the results presented above, we conclude that the magnetic domains comprising as-grown GaMnAs have similar magnetic anisotropy (predominantly cubic), thus resulting in a uniform behavior of the sample as a whole similar to the picture proposed in Ref. 15. In sharp contrast, domains in annealed GaMnAs films have a broad range of pinning fields (including even a nonzero probability of *negative* pinning fields) due to an increase in magnetic fluctuations,[7] indicating the presence of areas with various degrees of uniaxial anisotropy, which is in agreement with the mixed magnetic phase model proposed in Ref. 14. These results thus demonstrate that the magnetic nature of GaMnAs films can be represented either by a single (uniform) phase or by a mixed phase model, depending on the degree of magnetic anisotropy variation related to spatial magnetic fluctuations within the film.

ACKNOWLEDGMENTS

This work was supported by the Korea Science and Engineering Foundation (KOSEF) grant funded by the Korean government (MEST) (Grant No. R01-2008-000-10057-0), by the Seoul R&DB Program, by the Korea Research Foundation Grant No. KRF-2004-005-C00068, and by the National Science Foundation Grant No. DMR06-03762.

*slee3@korea.ac.kr

[1] G. A. Prinz, Science **282**, 1660 (1998).
[2] S. A. Wolf, D. D. Awschalom, R. A. Buhrman, J. M. Daughton, S. von Molnar, M. L. Roukes, A. Y. Chtchelkanova, and D. M. Treger, Science **294**, 1488 (2001).
[3] H. Ohno, D. Chiba, F. Matsukura, T. Omiya, E. Abe, T. Dietl, Y. Ohno, and K. Ohtani, Nature (London) **408**, 944 (2000).
[4] T. Hayashi, Y. Hashimoto, S. Katsumoto, and Y. Iye, Appl. Phys. Lett. **78**, 1691 (2001).
[5] B. S. Sorensen, P. E. Lindelof, J. Sadowski, R. Mathieu, and P. Svedlindh, Appl. Phys. Lett. **82**, 2287 (2003).
[6] K. W. Edmonds, K. Y. Wang, R. P. Campion, A. C. Neumann, N. R. S. Farley, B. L. Gallagher, and C. T. Foxon, Appl. Phys. Lett. **81**, 4991 (2002).
[7] K. W. Edmonds, P. Bogusławski, K. Y. Wang, R. P. Campion, S. N. Novikov, N. R. S. Farley, B. L. Gallagher, C. T. Foxon, M. Sawicki, T. Dietl, M. Buongiorno Nardelli, and J. Bernholc, Phys. Rev. Lett. **92**, 037201 (2004).
[8] S. J. Potashnik, K. C. Ku, S. H. Chun, J. J. Berry, N. Samarth, and P. Schiffer, Appl. Phys. Lett. **79**, 1495 (2001).
[9] K. M. Yu, W. Walukiewicz, T. Wojtowicz, I. Kuryliszyn, X. Liu, Y. Sasaki, and J. K. Furdyna, Phys. Rev. B **65**, 201303(R) (2002).
[10] K. Y. Wang, K. W. Edmonds, R. P. Campion, B. L. Gallagher, N. R. S. Farley, C. T. Foxon, M. Sawicki, P. Boguslawski, and T. Dietl, J. Appl. Phys. **95**, 6512 (2004).
[11] M. Sawicki, K. Y. Wang, K. W. Edmonds, R. P. Campion, C. R. Staddon, N. R. S. Farley, C. T. Foxon, E. Papis, E. Kamińska, A. Piotrowska, T. Dietl, and B. L. Gallagher, Phys. Rev. B **71**, 121302(R) (2005).
[12] A. Shen, H. Ohno, F. Matsukura, Y. Sugawara, N. Akiba, T. Kuroiwa, A. Oiwa, A. Endo, S. Katsumoto, and Y. Iye, J. Cryst. Growth **175-176**, 1069 (1997).
[13] X. Liu, Y. Sasaki, and J. K. Furdyna, Phys. Rev. B **67**, 205204 (2003).
[14] K. Hamaya, T. Taniyama, Y. Kitamoto, T. Fujii, and Y.

Yamazaki, Phys. Rev. Lett. **94**, 147203 (2005).
[15] K. Y. Wang, M. Sawicki, K. W. Edmonds, R. P. Campion, S. Maat, C. T. Foxon, B. L. Gallagher, and T. Dietl, Phys. Rev. Lett. **95**, 217204 (2005).
[16] U. Welp, V. K. Vlasko-Vlasov, X. Liu, J. K. Furdyna, and T. Wojtowicz, Phys. Rev. Lett. **90**, 167206 (2003).
[17] D. Y. Shin, S. J. Chung, S. Lee, X. Liu, and J. K. Furdyna, Phys. Rev. Lett. **98**, 047201 (2007).
[18] J. Kim, D. Y. Shin, T. Yoo, H. Kim, S. Lee, X. Liu, and J. K. Furdyna, J. Appl. Phys. **103**, 07D101 (2008).
[19] K. Okamoto, J. Magn. Magn. Mater. **35**, 353 (1983).
[20] H. X. Tang, R. K. Kawakami, D. D. Awschalom, and M. L. Roukes, Phys. Rev. Lett. **90**, 107201 (2003).
[21] S. J. Chung, D. Y. Shin, H. Son, S. Lee, X. Liu, and J. K. Furdyna, Solid State Commun. **143**, 232 (2007).
[22] E. C. Stoner and E. P. Wohlfarth, Philos. Trans. R. Soc. London, Ser. A **240**, 74 (1948).
[23] D. Y. Shin, S. J. Chung, S. Lee, X. Liu, and J. K. Furdyna, IEEE Trans. Magn. **43**, 3025 (2007).
[24] R. P. Cowburn, S. J. Gray, J. Ferre, J. A. C. Bland, and J. Miltat, J. Appl. Phys. **78**, 7210 (1995).
[25] G. J. Strijkers, S. M. Zhou, F. Y. Yang, and C. L. Chien, Phys. Rev. B **62**, 13896 (2000).